Interfacing Photonics to Free-Space via Large-area Inverse-designed Diffraction Elements and Metasurfaces

Alexander Yulaev,[1,2,3] Wenqi Zhu,[1,2,3] Chad Ropp,[1,2] Daron A. Westly,[1] Gregory Simelgor,[1] Cheng Zhang,[1,3] Henri J. Lezec,[1] Amit Agrawal,[1,2] and Vladimir A. Aksyuk[1]

[1]*Physical Measurement Laboratory, National Institute of Standards and Technology, Gaithersburg, Maryland 20899, USA*
[2]*Department of Chemistry and Biochemistry, University of Maryland, College Park, MD 20742, USA*
[3]*Maryland Nanocenter, University of Maryland, College Park, MD 20742, USA*

Abstract: Large-area inverse-designed photonic gratings and optical metasurfaces directly couple waveguides to wide free-space modes with custom wavefronts and polarizations in the visible and near-infrared. Design, modeling methods and experimental results are discussed.

1. Introduction and motivation

Better ways to couple integrated photonics to free-space can bring the benefits of miniaturization, low-cost mass production and complex system integration to optical applications requiring volumetric light-matter interaction. In one example, multiple advanced metrology methods use light to prepare and interrogate isolated atomic media [1-4]. Such techniques can find wider application spaces if complex free-space optics can be replaced by miniature, batch-fabricated, planar, integrated components [5].

However, addressing the full variety of such atomic systems requires efficient coupling from photonic waveguides to a wide range of free-space optical fields, spanning the length scales from sub-micrometer to centimeters and wavelength scales from blue/ultraviolet (UV) to near-infrared (NIR). The required wavefronts range from wide collimated beams at varying angles and polarization states for magneto-optical trapping [5,6] to diffraction-limited focal spots at high numerical apertures (NA) and up to millimeter-scale working distances for optical trapping and efficient coupling to individual atoms or ions. While in some cases smaller beams may be photonically generated and expanded to the required size via propagation through free-space or through bulk optics, in many cases this is either infeasible or undesirable due to the increased size and complexity. This motivates development of technologies for direct generation of these large-area free-space modes from planar photonics and, reciprocally, direct efficient coupling of light from these modes to on-chip nanophotonic waveguides [7,8].

While the optical frequencies range widely and multiple beams at different frequencies are often needed, for most of the atomic applications the frequencies are discrete, corresponding to specific atomic transitions. This is a good match for thin planar diffractive elements, such as photonic gratings and metasurfaces. Such devices can be efficient at one or a few specific target wavelengths, even though their chromatic dispersion is inherently difficult to minimize uniformly across broad spectral ranges for the wide free-space wavefronts.

Recently, inverse design, i.e., finding device structures that maximize performance using fully automated numerical optimization algorithms, has been used for successfully tackling a variety of photonics design challenges [9]. While it is conceptually appealing to apply this approach directly, the physical size of the problem that can be numerically solved is limited by the available computational resources. Therefore, we tackle the waveguide to free-space coupling design space by separating the problem into stages that are separately optimized by top-down and inverse design and combined to implement the desired function. Within this architecture we will discuss the specific design choices and experimental results.

We will describe an inverse design technique using deformable geometry and mesh implemented on a widely available commercial finite element software tool [8]. With this approach a judicious choice of parametrization of the geometry deformation can result in solutions that are novel, yet physically comprehensible and generalizable.

2. Design approaches and results

The devices we describe are linear and reciprocal, and we have used them experimentally for both projecting light into free-space and collecting light from free-space into single mode waveguides [4,8]. Since most of the experimental measurements are in the projection mode, we will use that to describe the device. The three sequential stages illustrated in Figure 1 are (Stage 1) the waveguide to photonic slab mode expansion creating a collimated wide Gaussian slab mode, (Stage 2) the photonic grating coupling to a collimated near-vertical free-space Gaussian and (Stage 3) the wavefront and polarization modification by an optical metasurface creating the surface-normal, focused, and elliptically polarized beam.

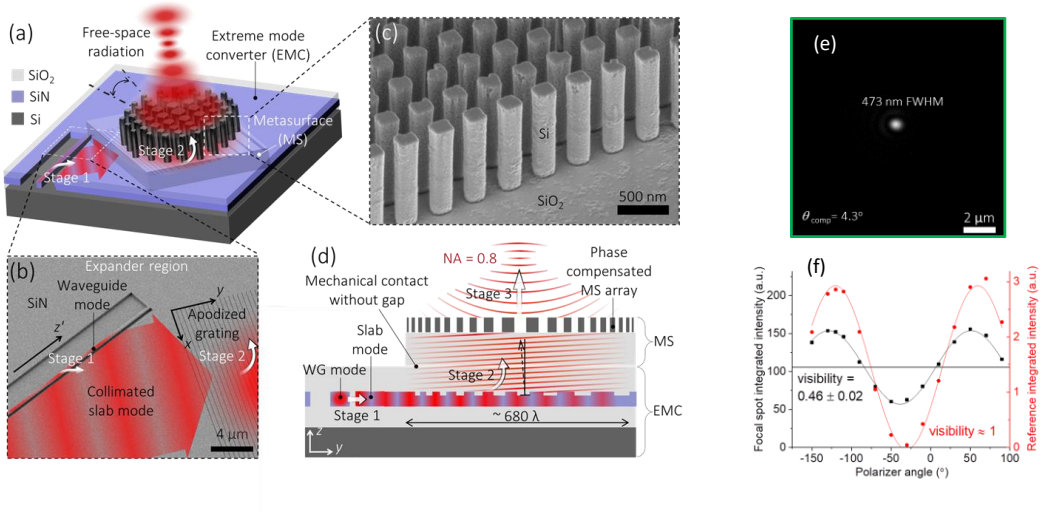

Figure 1. Planar photonics platform for flexible free-space coupling. (a) Three-stage approach for coupling high index photonic waveguide to free-space. (b) Stages one and two comprise evanescent coupling to a slab mode and vertical outcoupling by an apodized grating in the photonic layer. (c) In stage three a metasurface on a fused silica substrate modifies the free-space mode's wavefront and polarization. (d) Cross-sectional schematic illustrating high NA focusing in free space. (e) Diffraction limited 780 nm wavelength focal spot with NA ≈ 0.8 formed ≈ 75 μm away from the surface. The beam at the surface is a ≈ 200 μm full width at half maximum (FWHM) Gaussian. (f) Polarization is converted from linear after the stage-two grating (reference, red) to elliptical (focal spot, black) after the metasurface. Measurement one standard deviation statistical uncertainty is smaller than the symbol size. Adapted with permission from ACS Photonics 2019, 6, 11, 2902–2909. Copyright (2019) American Chemical Society.

In the first stage, evanescently coupling a straight photonic waveguide of a constant width to a photonic slab naturally produces a collimated slab mode, while we create a Gaussian intensity profile and outcouple all the light from the waveguide by appropriately apodizing the waveguide-slab gap. Other ways of expanding into the slab may be used, depending on the application requirements.

The problem of outcoupling a collimated slab mode with slowly varying intensity in the second stage is conveniently reduced from 3D to 2D, which simplifies the problem and makes the inverse design approach practical for even very long gratings (≈ 680 λ in the high-index SiN_x slab here). Rather than spatially varying the material permittivity, our inverse design approach starts from a uniform meshed grating, and proceeds to deform the model, creating spatially variable period and duty cycle. Other geometric parameters (grating depth, bottom cladding thickness) and the outcoupling beam angle and location are co-optimized. From a simple thin single-mode photonic slab grating layer light outcouples equally up and down. We chose to outcouple a collimated beam because for a given beam angle the bottom cladding thickness can be optimized to maximize upward power. A small negative diffraction angle provides efficient outcoupling into a single free-space diffraction order without unnecessarily decreasing critical dimensions. The outcoupled polarization is linear, and the device can be optimized for either transverse electric (TE) or transverse magnetic (TM) polarization.

In the third stage, light goes through the optical metasurface layer that can be designed to spatially modify the phase and polarization as desired [10]. Efficient metasurfaces have been fabricated by a variety of different techniques including direct etching and Damascene processes out of many low-loss high-index dielectric materials covering a broad wavelength range from NIR to deep UV [11]. The air-clad dielectric structures can be directly fabricated either on the top cladding of the integrated photonics or on their own transparent substrates, which are then integrated with the photonics. In the example in Figure 1, the metasurface corrects for the small beam angle coming from the grating, and produces a tightly focused spot, while also uniformly converting from linear to elliptical polarization. In principle, any desired functionality (amplitude, phase or polarization modulation) can be imprinted on the input beam during this third stage transformation.

While direct fabrication of the metasurface on photonics is conceptually simpler, the hybrid integration of metasurfaces with photonics adds free-space propagation distance between them through the thickness of the transparent metasurface substrate. This potentially enables using the metasurface to simultaneously process and combine beams projected onto it by multiple spatially separate photonic gratings. When these incident beams have different polarizations, the metasurface can perform completely independent wavefront change operations on them,

such as combining and projecting two input beams of different wavelengths into the same direction or the same focal spot.

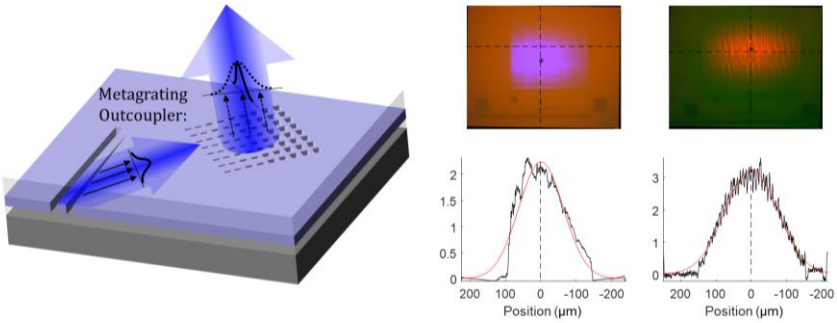

Figure 2. Large metagrating couplers. Elliptically shaped, collimated blue and red beams are generated by two metagrating devices on the same chip. Power profiles (black) are integrated over the vertical axes of the images and fitted with Gaussians (red).

Outcoupling large beams at short wavelengths present a challenge due to patterning and fabrication limitations, particularly when short and long wavelengths are combined. Relatively thick, high-index waveguides are desired for efficient confinement at the longer wavelengths, whereas blue outcoupling requires a combination of a short period and a weak scattering strength in the grating region. While shallow partially etched gratings can be used for reduced scattering strength, the etch depth is challenging to control with the desired accuracy. On the other hand, metagratings, where grating lines are replaced by linear arrays of subwavelength-sized fully etched boxes, can be designed to mimic the weakly scattering lines and achieve the desired range of scattering strengths for multiple wavelengths on the same chip. Figure 2 illustrates this approach and shows the corresponding experimental results. The presentation will cover these and other examples of large photonic grating couplers and their combination with metasurfaces for flexible and customized coupling between integrated photonics and free-space.

3. References

[1] J. Kitching, E. A. Donley, S. Knappe, M. Hummon, A. T. Dellis, J. Sherman, K. Srinivasan, V. A. Aksyuk, Q. Li, D. Westly, B. Roxworthy, and A. Lal, "NIST on a Chip: Realizing SI units with microfabricated alkali vapour cells," J. Phys.: Conf. Ser. **723**, 012056 (2016).

[2] K. K. Mehta, C. Zhang, M. Malinowski, T.-L. Nguyen, M. Stadler, and J. P. Home, "Integrated optical multi-ion quantum logic," Nature **586**, 533–537 (2020).

[3] R. J. Niffenegger, J. Stuart, C. Sorace-Agaskar, D. Kharas, S. Bramhavar, C. D. Bruzewicz, W. Loh, R. T. Maxson, R. McConnell, D. Reens, G. N. West, J. M. Sage, and J. Chiaverini, "Integrated multi-wavelength control of an ion qubit," Nature **586**, 538–542 (2020).

[4] M. T. Hummon, S. Kang, D. G. Bopp, Q. Li, D. A. Westly, S. Kim, C. Fredrick, S. A. Diddams, K. Srinivasan, V. Aksyuk, and J. E. Kitching, "Photonic chip for laser stabilization to an atomic vapor with 10^{-11} instability," Optica, OPTICA **5**, 443–449 (2018).

[5] D. J. Blumenthal, "Photonic integration for UV to IR applications," APL Photonics **5** (2), 020903 (2020).

[6] W. R. McGehee, W. Zhu, D. S. Barker, D. Westly, A. Yulaev, N. Klimov, A. Agrawal, S. Eckel, V. Aksyuk and J. J. McClelland, "Magneto-optical trapping using planar optics," New J. Phys. **23** 013021 (2021).

[7] A. Yulaev, W. Zhu, C. Zhang, D. A. Westly, H. J. Lezec, A. Agrawal, and V. Aksyuk, "Metasurface-Integrated Photonic Platform for Versatile Free-Space Beam Projection with Polarization Control," ACS Photonics, **6**, 2902–2909 (2019).

[8] S. Kim, D. A. Westly, B. J. Roxworthy, Q. Li, A. Yulaev, K. Srinivasan, and V. A. Aksyuk, "Photonic waveguide to free-space Gaussian beam extreme mode converter," Light: Science & Applications **7**, 72 (2018).

[9] S. Molesky, Z. Lin, A. Y. Piggott, W. Jin, J. Vucković, and A. W. Rodriguez, "Inverse design in nanophotonics". Nature Photonics, **12** (11), 659-670 (2018).

[10] A. Arbabi, Y. Horie, M. Bagheri, and A. Faraon, "Dielectric metasurfaces for complete control of phase and polarization with subwavelength spatial resolution and high transmission," Nat. Nanotechnology **10**, 937–943 (2015).

[11] C. Zhang, S. Divitt, Q. Fan, W. Zhu, A. Agrawal, Y. Lu, T. Xu, and H. J. Lezec, "Low-loss metasurface optics down to the deep ultraviolet region," Light: Science and Applications **9**, 55 (2020).